Colloid Polym Sci 277:1162–1171 (1999)

ORIGINAL CONTRIBUTION

M. Mosquet
Y. Chevalier
P. Le Perchec
A. Foissy
J.-P. Guicquero

The mechanism of fluidization of concentrated calcium carbonate slurries by poly(oxyethylene) diphosphonates

Received: 12 March 1999
Accepted in revised form: 2 July 1999

M. Mosquet · Y. Chevalier (✉)
P. Le Perchec
Laboratoire des Matériaux Organiques à Propriétés Spécifiques
LMOPS – CNRS, UPR 9031
B.P. 24, F-69390 Vernaison, France
e-mail: yves.chevalier@lmops.cnrs.fr
Tel.: +33-4-78022271
Fax: +33-4-78027187

A. Foissy
Laboratoire d'Électrochimie et des Systèmes Microdispersés
Université de Franche-Comté
UFR des Sciences et Techniques
F-25030 Besançon, France

J.-P. Guicquero
Lafarge Coppée Recherche
Laboratoire Central de Recherche, F-38297
Saint-Quentin-Fallavier, France

Abstract Nonionic poly(oxyethylene) polymers having a diphosphonate group at one chain end strongly adsorb onto $CaCO_3$ particles. The main consequence is a considerable lowering of the viscosity of concentrated slurries. This effect occurs because of the break up and redispersion of aggregates of flocculated $CaCO_3$ particles by the polymer adsorption. The mechanism of colloidal stabilization is steric, the particles becoming uncharged as the polymer adsorbs at their surface. As a consequence, the colloidal suspensions remain stable and fluid at high volume fractions and at high ionic strengths. On the other hand, because of the strong affinity of these polymers for $CaCO_3$ surfaces, the larger part of the polymer is adsorbed until the coverage of the particles reaches completion. The easy to handle polymer-to-solid weight ratio can then be used as a formulation parameter. The depletion flocculation by the nonadsorbed polymer is avoided.

Key words Polymer · Adsorption · Colloids · Stabilization · Poly(oxyethylene) diphosphonate

Introduction

New dispersants made of a nonionic hydrosoluble polymer [poly(ethylene oxide)] with a functional group having a strong affinity for mineral surfaces attached at one end of the macromolecular chains have recently been described [1–3]. The adsorption of these polymers on $CaCO_3$ as a model mineral surface and the rheological behavior of concentrated aqueous dispersions were studied as a function of the dispersant molecular structure, especially the functional group and the mass of the polymer, and conclusions about structure-properties relationships could be drawn. The diblock molecular architecture of the polymers allows a brushlike adsorption at the solid surface which differs from conventional homopolymer dispersants. An enhanced efficiency for the steric stabilization and for the fluidization of concentrated suspensions results from this macromolecular architecture [4, 5]. The diphosphonate end group has been selected as the most efficient for adsorption onto $CaCO_3$ [1–2]. These polymers proved superior to conventional dispersants such as polyacrylates [6, 7].

As a short summary of previous work [1–3], adsorption isotherms have shown that adsorption was ensured by the functional end group: pure poly(oxyethylene) did not adsorb by itself. As the coverage of the $CaCO_3$ particles by adsorbed polymer increased, the rheological behavior of the colloidal suspension turned from that of a viscous paste with a yield stress to that of a Newtonian liquid of low viscosity. The adsorption of the polymers took place as individual and independent macromolecules when the coverage was low. This was called the "mushroom" regime by Alexander [8] and de Gennes [9, 10]. A transition to a "brush" regime at higher coverage was observed where the adsorption isotherms leveled out because further adsorption was hindered by the presence of macromolecules which had already been adsorbed. The amount adsorbed did not depend on the macromolecular mass at low coverages and a dependence on the macromolecular mass appeared as the brush regime was reached. The full viscosity-lowering of the colloidal suspension was observed at this transition where the particle surface was completely covered by adsorbed polymer (Fig. 1). The amounts adsorbed and the concomitant viscosity-lowering were dependent on the type of functional group in the order carboxylate ≈ sulfonate < phosphonate < diphosphonate. Efficient fluidization required a minimum number of oxyethylene units of 20. There was no significant improvement on increasing further the molecular weight of the polymer.

The molecular parameters controlling the efficiency of polymeric dispersants with a di-block architecture could be identified. The adsorbed group at one of the macromolecular chain ends must have a strong affinity for the surface. The polymeric part should not adsorb on the surface and should be in good solvent conditions; it prevents particle aggregation when the surface is fully covered at the transition between the mushroom and the brush regimes. Based on the experimental observations, there is a clear relation between the viscosity-lowering and the adsorption ability of the polymer. The building up a steric barrier of adsorbed polymer brush, which acts against particle aggregation, was put forward as a mechanism [3].

In order to get more insight into the mechanism of the fluidization by adsorbed polymer, physical chemistry studies were carried out on colloidal suspensions of $CaCO_3$ stabilized by adsorbed poly(oxyethylene) diphosphonate. The results presented in this paper provide additional support for the mechanism of viscosity-lowering by de-aggregation of the clusters of $CaCO_3$ particles proposed in our previous papers. On the other hand, the present data underline the advantages of steric stabilization and of the nonionic character of the polymer for the stabilization at a high volume fraction of particles and/or at a high ionic strengths.

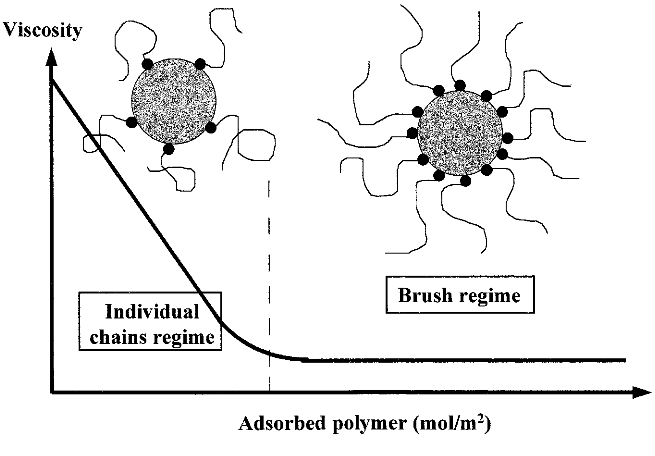

Fig. 1 Sketch of the viscosity dependence on polymer surface coverage

Materials and methods

Materials

The poly(oxyethylene) diphosphonate dispersants were synthesized by the Mannich–Moedritzer addition of formaldehyde and phosphorus acid to aminopoly(oxyethylene) [3, 11]. The anionic polymerization of ethylene oxide afforded a series of aminopoly(oxyethylene) compounds with narrow molecular mass distributions [11, 12]. The polymers are abbreviated as nEO-P2 where n stands for the number of ethylene oxide units ($2 < n < 100$).

The $CaCO_3$ was an additive-free calcite powder purchased under the trademark Socal 31 from Solvay. The dry powder consists of small particles of 70-nm mean diameter which are aggregated into flocs of large size and small density. The specific area as measured by the nitrogen Brunauer–Emmett–Teller method is 22 m^2/g.

$CaCO_3$ particles were suspended in water or in the polymer aqueous solutions and the samples were sonicated for 2 min with a Sonimasse high-power ultrasound device. After a first equilibration time, the pH was set at the desired value (most experiments were performed at pH 11) by addition of a small volume of concentrated sodium hydroxide and an equilibration time of 18 h at 20 °C was allowed to elapse before measurements were made.

Methods

Rheological measurements of concentrated $CaCO_3$ suspensions were performed in a Couette flow between coaxial cylinders with a Rheomat 30 rheometer from Contraves. The stress was obtained from measurements of the torque when a fixed shear rate was applied between two coaxial stainless steel cylinders. The suspension viscosity was calculated as the stress-to-shear-rate ratio. Applied shear rates were varied from 20 to 1708 s^{-1}.

Settling experiments were performed as follows. The suspensions containing 4 wt% $CaCO_3$ in water (and the dispersant to be studied) were shaken vigorously in order to ensure their homogeneity and were poured into graduated tubes. Settling under natural gravity was followed by recording as a function of time the level of the interface separating the clear supernatant and the milky sediment.

The sizes of the $CaCO_3$ (aggregated) particles were measured by means of quasielastic light scattering (QELS). The 20 wt% $CaCO_3$ suspensions were diluted to 0.01 wt% before each measurement. The dilutions were carried out with the aqueous phase of the 20 wt% dispersion in order to avoid desorption of the dispersant. Each dilution solution was the supernatant of the 20 wt% suspension under study, which was separated by ultracentrifugation with a Beckman JA21 centrifuge and filtered through a 0.2-μm membrane. The scattered light was measured as a function of time at a scattering angle of 90° with a Brookhaven device equipped with an argon ion laser working at a wavelength of 514.5 nm. The autocorrelation function of the scattered light was calculated by a digital correlator and the distribution of the translational diffusion coefficients was extracted by the nonlinear least-square method of the Brookhaven BI8000 software package. Particles diameters were calculated from the Stokes–Einstein relationship assuming a spherical shape. The experimental size distributions were essentially single-peaked and only mean values of the diameters, D, were retained.

Scanning electron microscopy was performed with a Jeol JSM-35 microscope. The dispersions were dried prior to the measurements in an oven at 40 °C; the dry powders were metalled with gold for their observation.

Electrophoretic mobilities were determined with a Rank–Brothers Mark2 device equipped with two platinum electrodes in a flat cell. The rates of the particles were measured by direct observations at one of the stationary planes with a camera. Consistent values of the velocities could be obtained by averaging ten measurements. The electrophoretic mobilities were calculated as the ratio of the particles mean velocity to the electric field.

The mechanism of fluidization by floc break up

Rheological behavior

The concentrated $CaCO_3$ dispersions in water are viscous pastes with a rheological behavior close to the behavior of a Bingham plastic body with a yield stress. The shear stress, τ, increases quite steeply as a function of the shear rate, $\dot{\gamma}$, at low values of the applied shear rate; however, the slope decreases drastically when high enough shear rates are applied. If the viscosity is defined as the ratio of the shear stress to the shear rate ($\eta = \tau/\dot{\gamma}$), the viscosity decreases as a function of the shear rate, which is a shear-thinning behavior. The existence of a stress threshold is difficult to assess, especially with the present rheometer working within the applied shear-rate mode. The flow curves were analyzed according to the Herschel–Bulkley relationship [13]

$$\tau = \tau_0 + K\,\dot{\gamma}^n \ . \tag{1}$$

The fit of this model to the experimental data (Fig. 2) was very good for the samples where some dispersant was present; however, this relationship was not correct in describing the flow behavior of the dispersant-free suspensions since the yield stress, τ_0, which gave the best agreement with the data was negative and large (about −300 Pa). The Herschel–Bulkley formula was then fitted to the nine data points in the high-shear-rate part of the data in order to retain a physically acceptable positive value for the yield stress. The poor agreement with the data in the low-shear-rate domain is noticeable in Fig. 2.

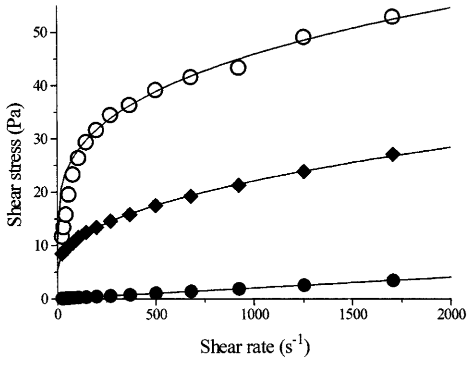

Fig. 2 Flow curves of 20 wt% aqueous suspensions of $CaCO_3$ particles at pH 11 as a function of the 50EO-P2 polymer content. The *solid lines* are the best fits of the Herschel–Bulkley relationship to the experimental data. The concentrations of 50EO-P2 polymer are 0 mmol/l (○), 0.25 mmol/l (◆) and 0.83 mmol/l (●)

Although a clear yield stress was not present, the Bingham plastic body model [13]

$$\tau = \tau_0 + \eta_P\,\dot{\gamma} \tag{2}$$

was also applied to the data because the yield stress and the plastic viscosity, η_P, which appear as parameters, have a clear physical meaning. The Bingham model did not fit the data for the low shear rates. A plastic viscosity could be defined in the high-shear-rate linear domain as the slope $\eta_P = d\tau/d\dot{\gamma}$ and was estimated as the slope of the linear portion of the flow curves. The yield stress was obtained by extrapolation of this linear portion to $\dot{\gamma} = 0$. The parameters of the Herschel–Bulkley and Bingham models are given in Table 1.

As the 50EO-P2 polymer is added to the $CaCO_3$ dispersion, the rheological behavior progressively turns into that of a Newtonian liquid of low viscosity (Fig. 2). The transformation of the suspension from a Bingham plastic body to a Newtonian liquid occurs by a progressive lowering of both the yield stress, τ_0, and the plastic viscosity, η_P, (Table 1). In the Herschel–Bulkley model, all the parameters also vary concomitantly as the 50EO-P2 concentration increases: the yield stress decreases towards zero, the exponent n approaches 1, and K tends towards the value of the Newtonian viscosity. Notice that both models are identical when $n = 1$. The Newtonian behavior is reached as the yield stress tends to vanishingly small values in both models.

This rheological behavior is characteristic of a weakly flocculated suspension which can be redispersed by the addition of dispersant [14–16]: a plastic flow with a yield stress for unstable colloidal dispersions at low dispersant contents turns into a Newtonian flow as the colloidal stability is improved by increasing the dispersant contents. Such behavior has often been observed when the colloidal stability of concentrated suspensions is varied. There are numerous examples in the literature [14–23] relating the emergence of a yield stress as the suspension is flocculated either by reaching the isoelectrical point, the critical coagulation concentration (ccc) of electrolyte or the critical flocculation temperature for electrostatically stabilized or sterically stabilized suspensions respectively, or by addition of a high-molecular-mass polymer. The rheological observations presented above are fully consistent with this behavior but do not establish definite proof of the fluidization mechanism, however. Strong repulsive interactions between colloidal particles also lead to plastic flow behavior in spite of their efficiency for ensuring colloidal stability. The yield stress increases strongly as the particles become ordered [24, 25] and the behavior of an elastic body is reached in colloidal crystals [26]. In this case, further enhancement of the stabilization would increase the yield stress. Our observations are the opposite: addition of polymer lowers the yield stress. The deaggregation mechanism of the fluidization is illustrated by several experiments in the following sections.

Sediment volumes

The volumes of the settled sediments were used as an investigation method for the structure of the aggregates of $CaCO_3$ particles. Flocs having an open porous structure of low density give rise to sediments of the same low density which occupy a large volume at the bottom of the sample after completion of their settlement. In contrast in the case of an efficiently stabilized dispersion of individual particles, the sediment is much more dense; close packing into a dense periodic structure could even be attained in cases of very slow settling [27–29]. Thus, the volume of the sediment provides a picture of the aggregation extent in suspensions of flocculated particles [16, 22]: the larger the sediment volume, the lower the sediment density.

The sediment volume patterns given by the $CaCO_3$ particle settlement experiments as a function of dispersant content (Fig. 3) give additional support to the mechanism of fluidization proposed on the basis of the rheological measurements. The sediment volumes are large for dispersant-free suspensions and decrease as the polymer content increases. The sediment volume can be reduced by a factor of 10 and reaches a constant value for polymer contents beyond a value corresponding to a polymer-to-$CaCO_3$ weight ratio of 5×10^{-3}–10^{-2}. The viscosity-lowering of the suspensions also remained constant when the polymer content was beyond this value (50EO-P2/$CaCO_3 \approx 1$ wt%) [2, 3]. The sediments are quite dense at high polymer contents; the sediment-to-$CaCO_3$ volume ratio reaches 3.5, corresponding to a volume fraction of $CaCO_3$ in the sediment of 30%. This density of the sediment is a mean value since the actual density in the sediment is not constant:

Table 1 Parameters of the Herschel–Bulkley and Bingham models of flow fitting to the experimental data as a function of the 50EO-P2 concentration

Concentration of 50EO-P2	Herschel–Bulkley			Bingham	
	τ_0(Pa)	K	n	τ_0 (Pa)	η_P (Pa s)
0, best fit to whole data	−300	2.85	0.0282	33.45	0.0117
0, best fit to the nine data points at high shear rate (see text)	10.5	3.94	0.318		
0.25 mmol/l	5.45	0.68	0.4625	13.8	0.0079
0.52 mmol/l	0.085	0.00325	0.9535	0.18	0.00225
0.83 mmol/l	0.03	0.0023	0.9833	0.015	0.00203
Newtonian flow for [50EO-P2] > 1 mmol/l	0	0.002	1	0	0.002

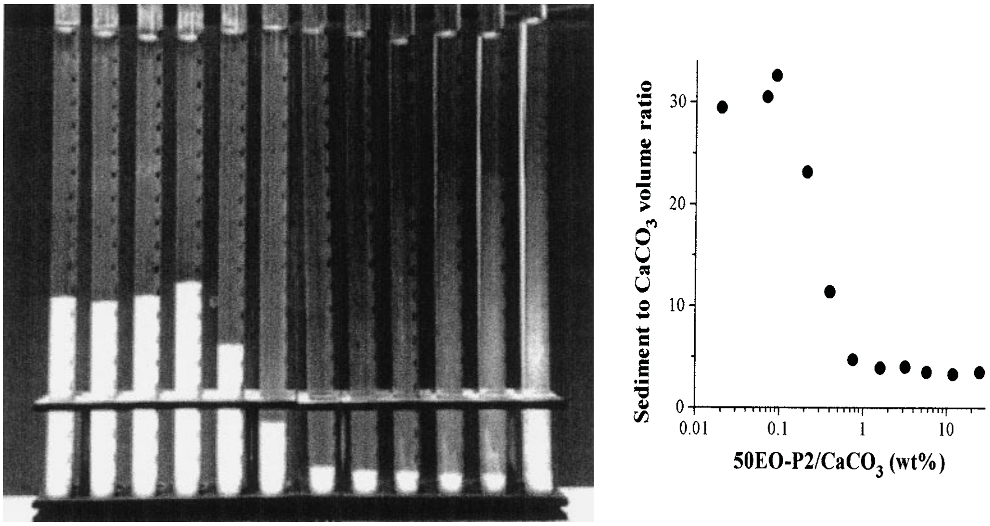

Fig. 3 Volume of $CaCO_3$ sediment after a 60 days' settling time as a function of the 50EO-P2 $CaCO_3$ weight ratio

the density increases with depth because the weight of the particles at the top of the deposit cause the particles at the bottom to be pressed together [27–29]. The maximum volume fraction in dense sediments corresponding to periodic close packing of individual particles is 50% [27]. Deaggregation of the primary particles by the polymer is then identified as the origin of the densification of the sediments as a function of the polymer content.

The rate of settlement also depends on the polymer content. Since the settlement measurements were performed with rather dilute suspensions (4 wt%), the viscosities were low and did not depend much on the dispersant content: the rates of settlement mainly depended on the size of the particles. Rapid settlement within few hours under natural gravity was observed for aggregates of particles because of their large size, while the same process took several days in the presence of large dispersant contents. The rates of settlement are also in agreement with the proposed picture of the mechanism of the action of the dispersants.

The efficiency of the dispersants can be evaluated from these simple settlement experiments. Rheological measurements have indicated that a minimum polymerization degree *n* of 20 was required for maximum viscosity-lowering [2]. The sediment volumes show the same trend (Fig. 4), but dense sediments can be obtained for polymers of slightly lower molecular mass ($n > 10$).

Light scattering measurements

The deaggregation of the flocs by the dispersant was monitored by means of particle size measurements. The size of the particles in diluted suspensions (0.01 wt%) was measured by means of QELS. Because this technique requires a high dilution of the particles, the concentrated dispersions (20 wt% $CaCO_3$) containing various dispersant contents were diluted to 0.01 wt% with the dispersing medium. A part of each sample was centrifuged in order to recover the supernatant, which is the dispersing medium in equilibrium with the adsorbed layer. This solution was used for the dilution of the concentrated suspension, keeping the adsorbed layer in equilibrium with the dispersing medium. This procedure avoided the desorption of the dispersant from the surfaces of the particles which would occur if the dilution was carried out with pure water. The autocorrelation functions of the scattered light were close to monoexponential and the diffusion coefficients could be converted into hydrodynamic diameters by assuming a spherical shape. The measurements of the dispersant-free suspension were of poor accuracy because of the fast settlement of the particles.

The experimental results show the deaggregation phenomenon quite unambiguously. The diameters decreased progressively from 3 μm to 400 nm as the dispersant was added (Fig. 5). The size of the particles remains constant for dispersant-to-$CaCO_3$ ratios above 10^{-2}, in the same range as for the rheology and sediment volume experiments [2, 3]. The diameter of the primary $CaCO_3$ particles as measured by electron microscopy of the dry powder is 70 nm. The constant size reached at high dispersant contents is higher by a factor of 6. The deaggregation of the particles by the dispersant is not complete. The measured diameter could be reduced to 200 nm by strong ultrasonic irradiation (the transducer was dipped into the dispersion for several hours) of the suspension in the presence of the dispersant. The origin of this difference may be the different averaging process sizes involved with these methods: the number average of the size is measured by electron microscopy while QELS gives the *z*-averaged size which is always larger that the number-average size (light scattering is more sensitive to the larger particles). The diameter measured by QELS should also be found to be larger than that of the primary particles because the thickness of the adsorbed polymer layer is included in the diameter. The contribution of the adsorbed layer to the size is

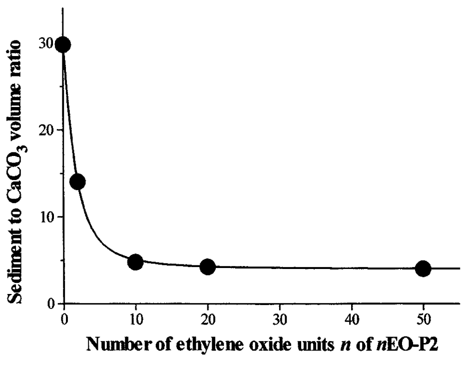

Fig. 4 Volume of sediment after a 60 days' settling time at high dispersant contents as a function of the polymerization degree *n*. $n = 0$ stands for a dispersant-free suspension

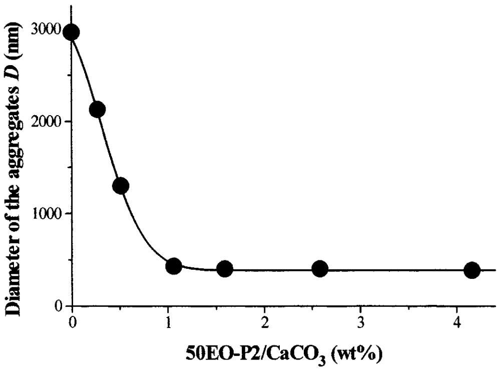

Fig. 5 Size of the clusters of $CaCO_3$ particles as measured by quasi elastic light scattering as a function of the 50EO-P2 dispersant content

expected to remain low since the radius of gyration of poly(ethylene oxide) having 50 monomer units in water is only of the order of 2 nm. It is then difficult to draw conclusions regarding the extent of the deaggregation process.

Electron microscopy observations

Lastly, the state of aggregation of the $CaCO_3$ particles could be visualised from their direct observation by scanning electron microscopy. This observation is called direct because pictures are obtained but the suspension had to be diluted in the same way as for the QELS experiments and was dried on the microscope grid prior to the observation. The structure of the aqueous suspension might not remain unaltered during drying; however, the pictures reveal aggregated structures of large size for the dispersant-free samples (Fig. 6a). These structures form a thick and porous film. The large thickness makes focusing difficult at high magnifications. Conversely, the suspensions dried in the presence of the 50EO-P2 dispersant give a thin film of small particles which are arranged in a more compact structure (Fig. 6b). These pictures display the structures which are expected on the basis of the sediment volume experiments: flocs of large size and of low density in the dispersant-free suspension turn into individual particles which settle into a dense sediment in the presence of dispersant.

Advantages of the steric stabilisation by nonionic polymers

The electrical charge of the $CaCO_3$ particles

The $CaCO_3$ particles are negatively charged at pH 11 since the isoelectrical point of calcite is 9.6 [30]. The electrokinetic potential depends on the Ca^{2+} activity according to the Nernst law [30], which is ideal behavior for a potential-determining ion. As the 50EO-P2 dispersant is added to the suspension, the measured electrophoretic mobility decreases and reaches vanishingly small values beyond a 50EO-P2/$CaCO_3$ weight ratio of 10^{-2} where the adsorbed polymer layer turns from the mushroom to the brush regime; thus, the surface potential at the shear plane is essentially zero when the particle surface is fully covered with the polymer. The $CaCO_3$ particles then behave as neutral

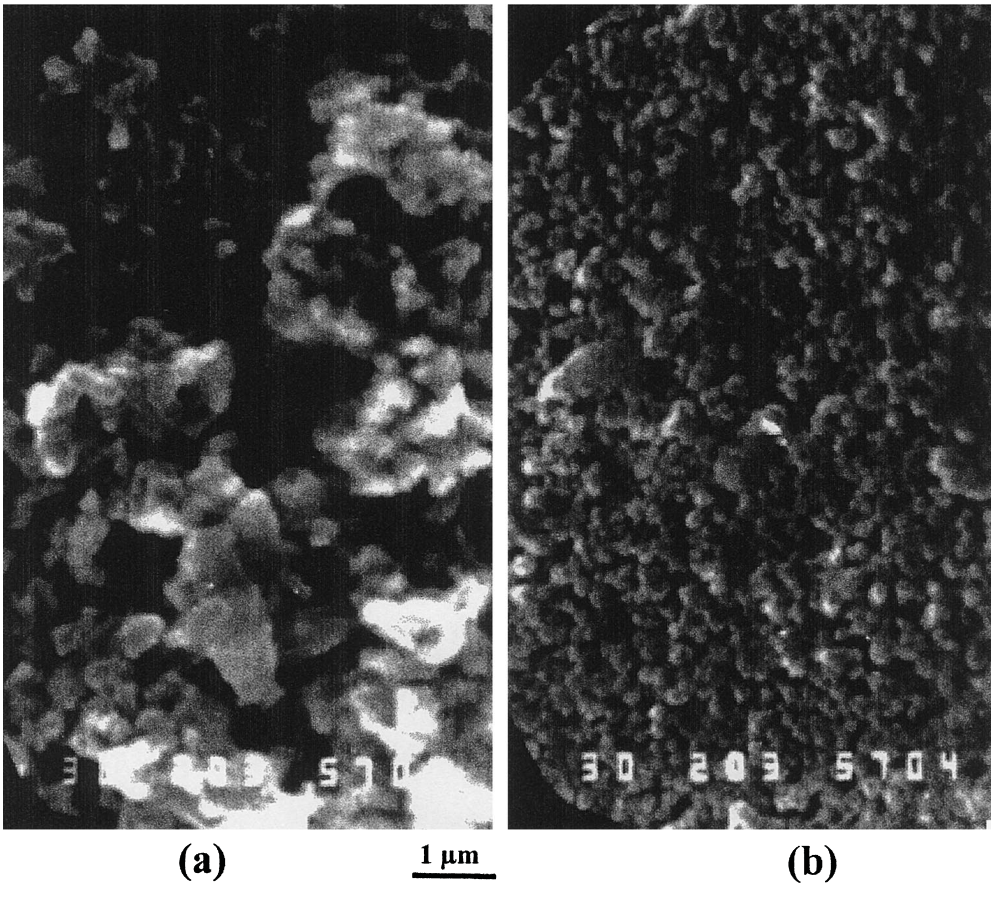

Fig. 6a, b Scanning electron microscopy pictures of $CaCO_3$ suspensions after drying. **a** Free of dispersant and **b** with 50EO-P2 particles. The mechanism of stabilization of the colloidal suspension progressively turns from electrostatic for the polymer-free suspensions to purely steric at high polymer contents. The crossover occurs at the mushroom-to-brush regime transition in the adsorbed layer. This observation is rather unexpected since the bare particles and the polymer are both negatively charged.

The origin of this effect may be the shear plane moving away from the $CaCO_3$ surface as the polymer adsorbs or the neutralization of the surface charge by the adsorption of cations. The electrokinetic potential measured at the shear plane should vanish when the adsorbed polymer layer thickness exceeds the Debye length. The mean thickness of the polymer layer in the mushroom regime is close to the radius of gyration of poly(ethylene oxide) having 50 monomer units; this is 2 nm [31]. The shift of the shear plane should be closer to the length of the fully extended chain, which is 20 nm. Values of the Debye length of 2 and 20 nm correspond to concentrations of divalent electrolyte of 10^{-2} and 10^{-4} mol/l, respectively. The actual ionic strength evaluated from the solubility of $CaCO_3$ in water at pH 11 [30], the concentrations of Na^+ and OH^- ions required to set the pH value at 11, and the Na^+ and $50EO\text{-}P2^{4-}$ ions from the dispersant (the part of it which is not adsorbed) fall in this range. An alternative origin of the very small electrokinetic potential may be the reduction in the surface charge by adsorption of cationic species. This would involve the concomitant adsorption of the diphosphonate polymer and Ca^{2+} ions. The adsorption of Ca^{2+} ions onto $CaCO_3$ particles is well documented: Ca^{2+} ions are indeed potential-determining ions [30], the adsorption is exothermic, and the heat of adsorption is −6.9 kcal/mol of Ca^{2+} [32]. The contribution of Ca^{2+} ions to the adsorption of acrylic polymers has also been evidenced and related to the formation of complex species between the polymer and Ca^{2+} ions in the solution [33, 34]. The same phenomena could be involved in the adsorption of the diphosphonate polymers since the complexing ability of the phosphonate groups for Ca^{2+} ions is high [35].

The shift of the plane of shear provides a correct rationale by itself but the adsorption of Ca^{2+} ions may also contribute to the lowering of the electrokinetic potential. The facts that the $CaCO_3$ particles become uncharged upon polymer adsorption and that the colloidal stability is ensured by steric repulsive forces has important consequences: these are discussed in the following sections.

The sensitivity to electrolytes compared to polyacrylates

Since the $CaCO_3$ particles are uncharged when the 50EO-P2/$CaCO_3$ weight ratio exceeds 1%, the interactions between the particles show very little sensitivity to the ionic strength. This is a considerable difference compared with the behavior of polyacrylates which bring about electrosteric interactions between the $CaCO_3$ particles.

The addition of electrolytes on suspensions stabilized by polyacrylates is twofold: a decrease in the electrostatic interactions between the particles on one hand, and a decrease in the electrostatic interactions between the polymer segments and the surface on the other hand. This second effect results in a collapse of the adsorbed polymer into a thin layer as the ionic strength is increased [6, 7]. The steric stabilization by polyacrylates then losses its efficiency when the polymer layer becomes thinner than the range of the attractive force between the particles.

There are no such electrostatic effects with the poly(oxyethylene) diphosphonates. A possible effect of electrolyte addition would be the modification of the solvent quality, i.e., of the solvation of the macromolecules in the adsorbed polymer layer; thus, pure water is a good solvent of poly(ethylene oxide) at room temperature and the quality of the solvent becomes poorer as the electrolyte concentration increases. This would result in a thinner polymer layer at high ionic strengths [4]. Since efficient steric stabilization can be achieved with 20EO-P2 (20 monomer units), the 100EO-P2 dispersant used for this experiment is oversized in its polymer block and the electrolyte addition is then inefficient in reducing the steric stabilization to a large enough extent. The absence of sensitivity towards electrolytes can be seen in the variation of the viscosity of concentrated $CaCO_3$ dispersions stabilized by 100EO-P2 and sodium polyacrylate (PANa) (molar mass = 5000 g/mol) studied for the sake of comparison (Fig. 8).

The abrupt increase in the viscosity of the suspension stabilized by the polyacrylate is caused by the flocculation of the particles when the $CaCl_2$ concentration exceeds ccc. The ccc is found to be around 3×10^{-2} mol/l.

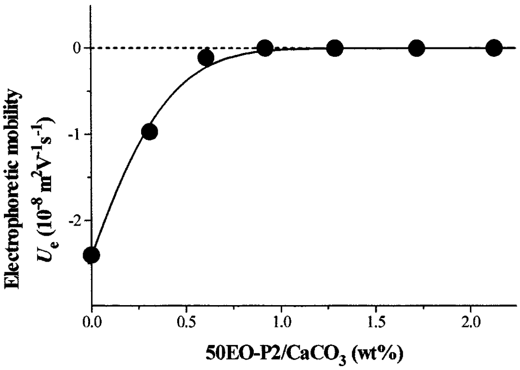

Fig. 7 Electrophoretic mobility of the $CaCO_3$ particles at pH 11 as a function of the 50EO-P2/$CaCO_3$ weight ratio

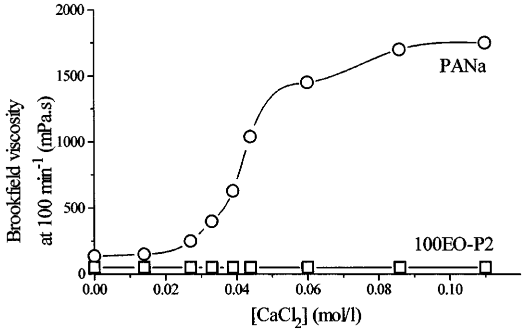

Fig. 8 Viscosity of $CaCO_3$ suspensions at 40 wt% measured with a Brookfield rheometer working at 100 rpm as a function of the concentration of $CaCl_2$ added. The dispersant contents are 1 wt% relative to $CaCO_3$ for both 100EO-P2 and sodium polyacrylate (PANa)

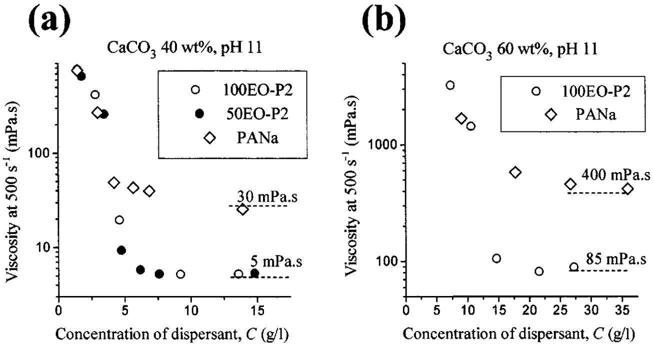

Fig. 9a, b Viscosity of concentrated slurries of $CaCO_3$ stabilized by poly(oxyethylene) diphosphonate dispersants compared to PANa. The measurements were performed at pH 11 and the viscosities are reported at a shear rate of 500 s^{-1}. **a**: 40 wt%; **b**: 60 wt%

The viscosity of the dispersion stabilized with the 100EO-P2 polymer is constant in the $CaCl_2$ concentration range studied. The electrolyte concentration required for the destabilization of the particles stabilized with the polyacrylate is too low to change significantly the thickness of the 100EO-P2 layer.

Stabilization of slurries at high volume fractions of $CaCO_3$

The rheological behavior of concentrated slurries at pH 11 was studied and compared to that of the same polyacrylate mentioned in the previous sections. With the 100EO-P2 dispersant, the same qualitative behavior as for the suspensions of 20 wt% $CaCO_3$ was observed for suspensions of 40 and 60 wt% $CaCO_3$: the flow turned from that of a plastic body to a Newtonian behavior as the dispersant content increased. In contrast, the values of the yield stress remained at a high level when the polyacrylate was used in the same concentration range as 100EO-P2. The viscosities of 40 and 60 wt% slurries of $CaCO_3$ stabilized by *n*EO-P2 dispersants and PANa are compared in Fig. 9. Given the same dispersant content expressed in mass of dispersant, the viscosities of the suspensions stabilized by the PANa polyelectrolyte are larger in all instances. When the dispersant contents are high enough for the viscosity to be independent of the dispersant concentration, the viscosities reached with 100EO-P2 are lower by a factor of 5–6 than with PANa.

This difference in the rheological behavior is due to the difference in the stabilization mechanism. The 100EO-P2 dispersant is able to deagglomerate the flocs of $CaCO_3$ particles efficiently and to provide stabilization by means of short-range steric repulsive forces, which remain active at high volume fractions of particles. In contrast, the polyacrylate acts by an electrostatic stabilization mechanism which is inefficient in concentrated media. Moreover, the binding of the polyacrylate to the $CaCO_3$ surface is weaker than that of the diphosphonate. This lesser affinity can be compensated for by using higher concentrations of dispersant in the cases where the volume fraction of $CaCO_3$ in the dispersions remains moderate. An incomplete coverage of the surface by the polymer is not fatal because the electrostatic interactions between the particles are long-ranged; however, incomplete coverage of the surface cannot ensure efficient colloidal stabilization in concentrated slurries because the short mean distance between particles necessarily implies short-range interactions.

The effect of nonadsorbed polymer

The presence of nonadsorbing polymer in the aqueous phase of colloidal suspensions is known to give rise to attractive interactions between the particles [4, 36, 37]. The origin of such attractions is the osmotic pressure gradient between the bulk polymer solution and the depletion layer at the surface of the particles. This phenomenon may lead to the coagulation of the particles which is known as "depletion flocculation" [4]. Even in the case of an adsorbing polymer, the fraction of the polymer which is not adsorbed raises the osmotic pressure in the bulk aqueous phase. The consequence is an attraction between the particles which acts as a supplementary interaction with respect to the hypothetical case where the whole polymer adsorbs [38]. On this basis, a strong adsorption of the polymer which allows a low concentration of free polymer in the bulk aqueous phase is an obvious benefit as regards the colloidal stabilization.

The adsorption of the *n*EO-P2 dispersants is very strong [1–3], and so the concentration of free polymer remaining in the aqueous phase, at thermodynamic equilibrium with the adsorbed polymer layer, is very low until the whole surface of the particle is covered. In these conditions, the fraction of polymer adsorbed is 95% (Fig. 10); the exhaustion of the solution by the adsorption is very close to completion. When the transition to the brush regime is reached by increasing the polymer concentration, the adsorption of additional macromolecules is hindered by the ones already adsorbed [3], and the concentration of polymer in equilibrium with the adsorbed layer starts to increase (Fig. 10).

The fact that the fraction of adsorbed polymer is close to 1 allows the use of the dispersant-to-$CaCO_3$ weight ratio as a practical formulation parameter. Indeed, the surface excess in the adsorbed polymer layer, which actually controls the rheological properties of the suspensions, is directly related to this ratio since the whole polymer is adsorbed. The dispersant-to-$CaCO_3$ weight ratio required for a given surface excess remains identical whatever the $CaCO_3$ content of the dispersion, which makes this ratio the relevant parameter in practical applications. If the adsorption was not so strong, the assumption of full adsorption could not be made because the surface excess would depend on the $CaCO_3$ content of the slurries. In the brush regime where the adsorption is not complete, the surface excess depends again on the $CaCO_3$ content, but this situation is not interesting in practical uses since there is no further lowering of the viscosity in this regime.

As the free polymer concentration increases in the brush regime of adsorption, the colloidal stability of the $CaCO_3$ particles is expected to alter and a slight increase in the viscosity of the suspensions of $CaCO_3$ is actually observed (Fig. 11). This observation is ascribed to the partial aggregation of $CaCO_3$ particles by the free polymer. There is, however, no definite proof for this explanation. The observed increase in viscosity is much larger than the increase in viscosity of the aqueous phase alone by the same concentration of free polymer.

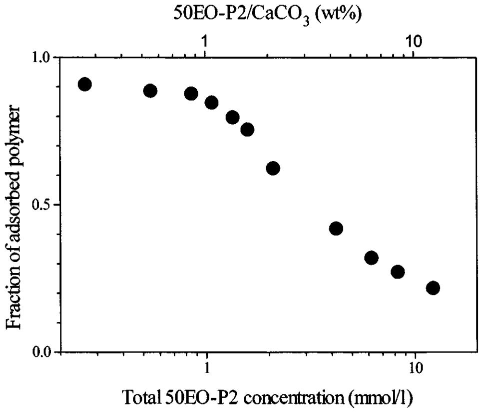

Fig. 10 Fraction of 50EO-P2 polymer adsorbed on $CaCO_3$ for a 20 wt% dispersion as a function of the polymer content expressed as the total concentration (*bottom* *x*-axis) or as the dispersant/$CaCO_3$ weight ratio (*top* *x*-axis)

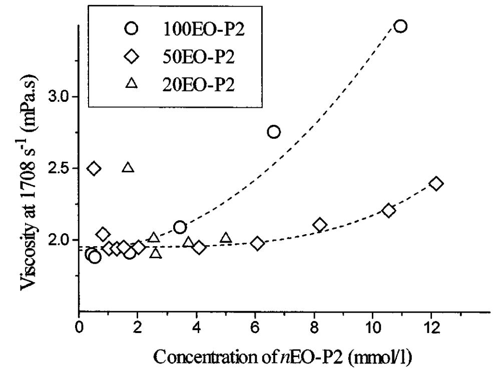

Fig. 11 Viscosity of 20 wt% $CaCO_3$ dispersions at pH 11 and 1708 s^{-1} shear rate as a function of the 50EO-P2 concentration (the *vertical scale* is expanded in the domain of low viscosities)

The increase in viscosity is not large and the flow behavior of the suspensions remains Newtonian, but an excess of polymer clearly has a disastrous influence. The correct choice of the polymer concentration makes sense and the availability of an easy-to-handle formulation parameter such as the dispersant-to-$CaCO_3$ weight ratio appears quite useful.

Conclusions

The present results suggest supplementary materials to these from our previously reported studies on functional poly(oxyethylene)s dispersants which were mainly directed towards structure activity relationship [1–3]. Firstly, the present physical chemistry studies provide further support to the mechanism of fluidization by floc break up. Secondly, they provide new insights into the action of the poly(oxyethylene) diphosphonate dispersants.

Experimental data from rheology, sediment volumes, light scattering, and electron microscopy agree with each other in identifying the deaggregation of clusters of $CaCO_3$ particles (flocs) as the origin of the fluidization of concentrated aqueous slurries of $CaCO_3$ by the dispersant. In particular, the measurements of the size by means of QELS show unambiguously the reduction in the floc diameter as a function of the dispersant content. The yield stress observed in the flow behavior of the dispersions is associated with the presence of clusters of primary particles. Two regimes can be clearly distinguished according to the dispersant content. At low dispersant contents, where the surface of the particles cannot be fully covered by the adsorbed polymer, the deaggregation is not complete, the dispersions are quite viscous, and the flow behavior displays a yield stress. The coverage of the particle surface reaches completion at the transition from the "mushroom" to the "brush" regime [1–3] as described by Alexander [8] and de Gennes [9, 10]. Beyond this coverage, the flow of the suspensions is Newtonian, even at high fractions of $CaCO_3$ (60 wt%), the viscosity is low, and the size of the particles becomes close to (but significantly higher) that of the primary particles. The adsorption isotherms [3] have shown that the crossover between these two regimes takes place at a dispersant-to-$CaCO_3$ weight ratio of 10^{-2}, and all the data obtained by means of the different techniques point out the same dispersant-to-$CaCO_3$ weight ratio as the magnitude of the transition with a nice convergence.

The nonionic character of the polymers makes the stabilization mechanism purely steric; the electrokinetic mobility of the particle is zero in the presence of polymer. This type of stabilization allows the efficient fluidization of concentrated slurries, even in the presence of electrolytes. The comparison with PANa shows the superiority of the steric stabilization in such cases.

Lastly, the affinity of the dispersant for the surface of the particles is an important parameter. In the present case, where the full polymer is adsorbed until complete coverage of the surface, the effect of the nonadsorbing polymer can be avoided. A further advantage is the possible use of the dispersant-to-$CaCO_3$ weight ratio as the main formulation parameter. The optimum properties are attained at the same dispersant-to-$CaCO_3$ weight ratio, whatever the $CaCO_3$ content, which is quite convenient in practice.

References

1. Mosquet M, Chevalier Y, Le Perchec P, Guicquero J-P (1997) New J Chem 21: 143
2. Mosquet M, Chevalier Y, Brunel S, Guicquero J-P, Le Perchec P (1997) J Appl Polym Sci 65: 2545
3. Chevalier Y, Brunel S, Le Perchec P, Mosquet M, Guicquero J-P (1997) Prog Colloid Polym Sci 105: 6
4. Napper DH (1983) Polymeric stabilization of colloidal suspensions. Academic Press, London
5. Fleer GJ, Cohen Stuart MA, Scheutjens JMHM, Cosgrove T, Vincent B (1993) Polymers at interfaces. Chapman & Hall, London
6. Rogan KR, Bentham AC, Beard GWA, George IA, Skuse DR (1994) Prog Colloid Polym Sci 97: 97
7. Rogan KR, Bentham AC, George IA, Skuse DR (1994) Colloid Polym Sci 272: 1175
8. Alexander S (1977) J Phys 38:983
9. de Gennes PG (1980) Macromolecules 13: 1069
10. de Gennes PG (1987) Adv Colloid Interface Sci 27: 189
11. Mosquet M (1994) PhD thesis. University of Lyon
12. Mosquet M, Chevalier Y, Le Perchec P, Guicquero J-P (1997) Macromol Chem Phys 198: 2457
13. Hunter RJ (1989) Foundations of colloid science vol II. Clarendon Oxford, pp 992–1052
14. Tadros ThF (1992) Pure Appl Chem 64: 1715
15. Le Bars N, Tinet D, Faugère AM, Van Damme H, Levitz P (1991) J Phys III 1: 707
16. Le Bars N, Levitz P, Messier A, François M, Van Damme H (1995) J Colloid Interface Sci 175: 400
17. Dobiáš B (ed) (1993) Coagulation and flocculation. Dekker, New York
18. Leong Y-K, Boger DV, Scales PJ, Healy TW, Buscall R (1993) J Chem Soc Chem Commun 639
19. Liang W, Bognolo G, Tadros ThF (1995) Langmuir 11: 2899
20. Otsubo Y (1992) Langmuir 8: 2336
21. Liu SF, Lafuma F, Audebert R (1994) Colloid Polym Sci 272: 196
22. Mange F, Couchot P, Foissy A, Pierre A (1993) J Colloid Interface Sci 159:58
23. Tadros ThF (1989) Prog Colloid Polym. Sci 79: 120
24. Liang W, Tadros ThF, Luckham PF (1992) J Colloid Interface Sci 153:131
25. Tadros ThF, Liang W, Costello B, Luckham PF (1993) Colloids Surf A 79: 105
26. Chen L-B, Zukoski CF (1990) J Chem Soc Faraday Trans 86: 2629
27. Smits C, Van Duijneveldt JS, Dhont JKG, Lekkerkerker HNW, Briels WJ (1990) Phase Transitions 21: 157
28. Emmett S, Lubetkin SD, Vincent B (1989) Colloids Surf 42: 139
29. Lubetkin SD, Wedlock DJ, Edser CF (1990) Colloids Surf 44: 139
30. Pierre A, Lamarche JM, Mercier R, Foissy A, Persello J (1990) J Dispersion Sci Technol 11: 611
31. Devanand K, Selser JC (1991) Macromolecules 24: 5943.
32. Huang YC, Fowkes FM, Lloyd TB, Sanders ND (1991) Langmuir 7: 1742
33. El Attar Sofi Y, Carquille C, Lamarche JM, Foissy A (1990) Prog Colloid Polym Sci 82: 43
34. Dupont L, Foissy A, Mercier R, Mottet B (1993) J Colloid Interface Sci 161: 455
35. Tomson MB, Kan AT, Oddo JE (1994) Langmuir 10: 1442
36. Asakura S, Oosawa F (1954) J Chem Phys 22: 1255
37. Asakura S, Oosawa F (1958) J Polym Sci 33: 183
38. Cowell C, Li-in-on R, Vincent B (1978) J Chem Soc Faraday Trans I 74: 337